공학석사 학위논문

Prediction of Mechanical Behavior of Explosive Welded Bulk Clad Material

폭파용접으로 제작된 두꺼운 이종결합 재료의 역학적 거동 예측

2014년 2월

서울대학교 대학원

재료공학부

홍 종 화

Prediction of Mechanical Behavior of Explosive Welded Bulk Clad Material

지도 교수 정 관 수

이 논문을 공학석사 학위논문으로 제출함
2013년 10월

서울대학교 대학원
재료공학부
홍 종 화

홍종화의 공학석사 학위논문을 인준함
2014년 1월

위 원 장 한 흥 남 (인)

부위원장 정 관 수 (인)

위 원 유 웅 렬 (인)

Prediction of Mechanical Behavior of Explosive Welded Bulk Clad Material

Advisor: Kwansoo Chung

by

Jong-Hwa Hong

Submitted for the Degree of Master

2014

Department of Materials Science and Engineering
The Graduate School
Seoul National University

Abstract

Prediction of Mechanical Behavior of Explosive Welded Bulk Clad Material

Jong-Hwa Hong
Department of Materials Science and Engineering
The Graduate School
Seoul National University

The objectives of this thesis is to predict the mechanical behavior of bulk clad metal welded by explosion. The clad is composed of corrosion resistant alloy coating and stainless steel 316 affiliation.

Commonly bulk clad material is used as a structural material experiencing warm temperature. It is important for clad combined more than two different thermal expansion coefficients to be measured separately in location when thermal analysis evaluation is implemented. However this locally separated specimen should be confirmed whether it represents the whole clad material behavior properly. To measure the whole mechanical behavior of bulk clad material, unusual specimen shape was designed. This thesis attempts to predict the whole mechanical behavior from divided partial properties.

Consequently, individual properties can predict the whole mechanical behavior not only short deformation range but also large deformation range at room temperature and warm temperature very well.

Keywords: Explosive welding, Bulk, Clad, Warm temperature, Mechanical behavior
Student Number: 2012-20642

Contents

List of Tables

List of Figures

Chapter 1. Introduction

Explosive welding is a solid state process to join two or more metals together under high impact pressure using explosion force. This welding method can be applied to weld similar materials like usual welding process. However its major industrial potential lies in the fact that it may use to clad dissimilar materials, many of which are impossible to be joined by any other methods beforehand. [1]

There are some terminologies in the explosive welding process. An anvil is the surface on which the base plate rests. The base metal is indicated as a parent material, base plate and backer. Above the base plate, another plate maintains specific distance before joining operation occur. The distance is called stand-off and the plate is called as clad, clad layer, cladder and coating. Clad is also used as a verb which means joining metals together. Above the coating, explosive is present and detonates from the corner of the coating. [2]

There are numbers of advantages of the explosive welding process over competing processes. Above all, it has no heat-affected zone (HAZ), no diffusion and it just melts locally in a minor place. In addition, it doesn’t stand in the way of being the final product although melting temperatures and the thermal expansion coefficient of each materials are difference. This process is used on commercial scale because of its low cost factor. Moreover we don’t need to prepare surfaces for this type of welding operation. Lastly the most important advantage is its possibility to join the metal together which would usually be incompatible each other, for instance aluminium, zirconium,

titanium, tungsten, nickel and copper with steel and so forth.

Despite of several advantages, there are still some disadvantages. This can’t be applied to brittle materials. Also it has to be a special shapes such as plates and cylinders.

The clad metals have widely applied in constructional, chemical shipbuilding industry. The products made by explosive welding are used as pipes to heat exchanger, pressure vessels, paper machines, clad tubes, aerospace structures, bi-metal sliding bearings, corrosion resistant chemical tanks and offshore applications.

In this thesis, corrosion resistant alloy and stainless steel cladded by explosive welding is investigate. Roughly 27mm to 28mm clad panel which is composed of 25mm SUS316 and 3mm corrosion resistant alloy coating is welded.

The uni-axial tension is one of the simple test to notice the mechanical properties of materials but it is difficult to perform the test for dissimilar welded bulk material using universal test machine on account of its heavy thickness. In the case of homogeneous bulk metals, it is no matter for one to measure any location of its properties because the any cut part can represents entire properties of bulk materials. However for inhomogeneous bulk metals such as clad or composite their whole properties are difficult to be measured because the properties are changing from measured place, which can’t represent the whole properties. During the explosive processing, the mechanical properties of cladded material are changed over all, especially in near the interface the cladded material undergoes substantial changes. That’s

why one partial properties can’t represent the general properties of the cladded material.

The aim of this thesis is to predict the whole simple tension behavior of bulk cladded metal from the partially measured results with the simulation of ABAQUS/Standard. The jobs are performed in two different temperature atmospheres, the one is in room temperature and the other is in 300℃. To verify the entire mechanical properties of cladded metal, a new specimen shape is designed. With this specimen one can measure the whole mechanical properties of inhomogeneous bulk metal at once. The reason to divide the clad material for each location is to perform the thermal analysis evaluation. Since explosive welded material has dissimilar thermal expansion coefficients, the residual stress exists on metal bonded interface. The different extension may cause severe problems. So when one designs structure with bulk clad material in the changing heat atmosphere should consider the possibility of the matters. It can’t be denied that partial properties are very important in the case of thermal analysis with the inhomogeneous metal. This thesis is started from this idea. Although the residual stress doesn’t come into sight in this thesis, one may further research an investigation of this. In this dissertation, it is restricted only to predict the simple tension behavior of bulk clad material assuming the virgin material originally.

Chapter 2. Theory

2.1 The curve conversion

Experiment gives the engineering data after uni-axial tension test is finished. Plotted data which are presented in engineering stress-engineering strain curve should be converted into true stress-true strain curve because stress and strain are calculated by initial measurement in engineering space. The converting method of the simple tension or uni-axial tension is described below. [3]

To describe the uni-axial tension test, engineering stress and engineering strain should be defined. The engineering stress is

$$\sigma^n = \frac{F}{A_0} \tag{1.1}$$

and the engineering strain is

$$d\varepsilon^n = \frac{dl}{l_0} \; or \; \varepsilon^n = \frac{l - l_0}{l_0} \tag{1.2}$$

where F is applied axial force. A_0 and l_0 are initial cross section area and initial length of the specimen respectively. The superscript n stands for nominal which is usually used as same meaning with engineering stress.

Actually the engineering stress and engineering strain are not a true value

because it is defined in terms of the original dimensions. As an alternative, true stress and true strain which is also called logarithmic strain is described as following Eqns.(1.3) and (1.4) respectively. The equations consider the changing area and length during the test that is why it is called ‘true’ stress, and ‘true’ strain.

$$\sigma^t = \frac{F}{A} \tag{1.3}$$

$$d\varepsilon^t = \frac{dl}{l} \; or \; \varepsilon^t = \int_{l_0}^{l} \frac{dl}{l} = \ln \frac{l}{l_0} \tag{1.4}$$

where A is the deformed area and l is the deformed length of the specimen. The incompressibility is usually assumed based on the experimental results during the plastic deformation. Incompressible volume are that the initial volume don’t change after deformation.

$$A_0 l_0 = Al \tag{1.5}$$

Using the Eqns.(1.1) and (1.3), the following relationship can be easily obtained with incompressibility.

$$\sigma^t = \sigma^n \frac{A_0}{A} = \sigma^n \frac{l}{l_0} \tag{1.6}$$

From the Eqn.(1.6) with Eqn.(1.2), true stress is expressed in engineering

stress and engineering strain.

$$\sigma^t = \sigma^n \frac{l}{l_0} = \sigma^n (1 + \varepsilon^n) \quad \textbf{(1.7)}$$

Using Eqn.(1.2) and Eqn.(1.4), engineering and true strain relationship can be obtained.

$$\varepsilon^t = \ln \frac{l}{l_0} = \ln(1 + \varepsilon^n) \quad \textbf{(1.8)}$$

Hence the Eqn.(1.8) is

$$\varepsilon^n = e^{\varepsilon^t} - 1 \quad \textbf{(1.9)}$$

Engineering stress-engineering strain curve can be converted into true stress-true strain using Eqn.(1.7) and (1.9) sequentially. One can get another equation of (1.7) as a result of Eqn.(1.9).

$$\sigma^t = \sigma^n e^{\varepsilon^t} \quad \textbf{(1.10)}$$

The ratio of engineering stress to true stress is

$$\sigma^n : \sigma^t = 1 : e^{\varepsilon^t} \quad \textbf{(1.11)}$$

or

$$\sigma^n : \sigma^t = 1 : (1 + \varepsilon^n) \qquad \textbf{(1.12)}$$

We get the all the equations to obtain true stress-true strain relationship.

First of all, using the proportional expression in Eqn.(1.12), one can get the relationship between true stress-engineering strain from engineering stress-engineering strain described in Fig. 2.1. That is, true stress-engineering strain behaves higher than engineering stress-engineering strain.

Then, considering only strain, one notices that true strain is smaller than originally used engineering strain. This is because the length l used as denominator is increasing during deformation for true strain although the denominator of the engineering strain are constant for the uni-axail test. The result makes the true stress-true strain curve higher than true stress-engineering strain curve as following the Fig. 2.2.

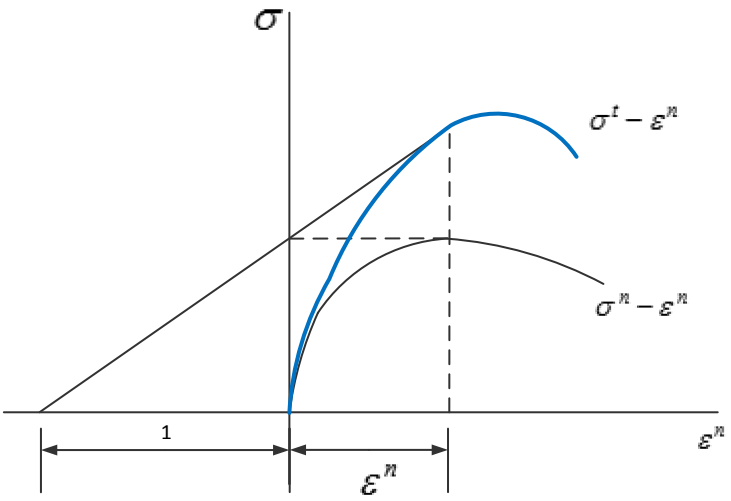

Fig. 2.1 Conversion from engineering stress-engineering strain to true stress-true strain

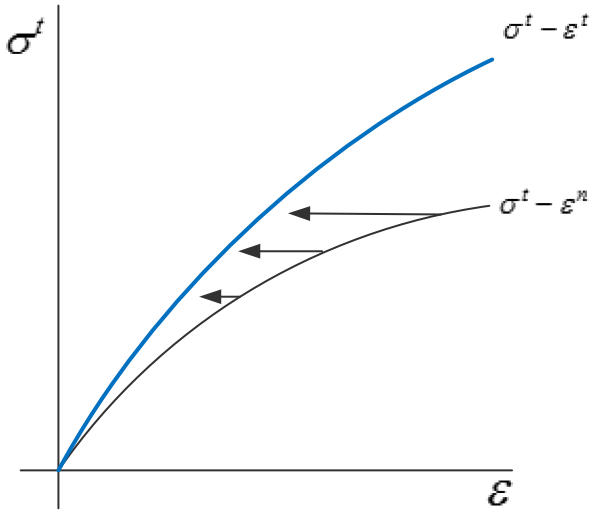

Fig. 2.2 Comparison engineering stress-engineering strain curve with engineering stress-true strain curve

For the engineering curve, Eqn. (1.13) gives onset point of non-uniform deformation. The point is called the ultimate tensile strength (UTS).

$$\frac{d\sigma^n}{d\varepsilon^n} = 0 \qquad \textbf{(1.13)}$$

From (1.10) one obtains

$$\sigma^n = \sigma^t e^{-\varepsilon^t} \qquad \textbf{(1.14)}$$

applying Eqn.(1.14) and Eqn.(1.8) to Eqn.(1.13). Then, one gets

$$\frac{d\sigma^n}{d\varepsilon^n} = \frac{d\sigma^n}{d\varepsilon^t}\frac{d\varepsilon^t}{d\varepsilon^n} = \left(\mathrm{e}^{-\varepsilon^t} \frac{d\sigma^t}{d\varepsilon^t} - \mathrm{e}^{-\varepsilon^t} \sigma^t \right) \frac{1}{1+\varepsilon^n} = \left(\frac{d\sigma^t}{d\varepsilon^t} - \sigma^t \right) \mathrm{e}^{-2\varepsilon^t} = 0$$

To satisfy above equation, only this following is possible.

$$\frac{d\sigma^t}{d\varepsilon^t} = \sigma^t \qquad \textbf{(1.15)}$$

which is the start point of the instability for true stress-true strain curve corresponding to Eqn.(1.13).

2.2 Hardening laws

After converting engineering stress-engineering strain, hardening curve should be retained to describe the plastic properties. Despite of plastic deformation state, the total strain is not a pure plastic strain but the sum of elastic strain and plastic strain under the monotonous proportional loading condition. For instance in Fig. 2.3 total strain of point Q is sum of elastic strain and plastic strain as shown in Eqn.(1.16)

$$\varepsilon = \varepsilon^e + \varepsilon^p \tag{1.16}$$

To obtain the plastic strain, total stain should be subtracted by elastic strain in below.

$$\varepsilon^p = \varepsilon - \varepsilon^e \tag{1.17}$$

In the assumption of Hooke's law. Eqn.(1.17) becomes

$$\varepsilon^p = \varepsilon - \frac{\sigma}{E} \tag{1.18}$$

Then the true stress-true strain curve in Fig. 2.3 becomes Fig. 2.4. The point P is located on the y-axis because the plastic strains are zero until it reaches the yield stress.

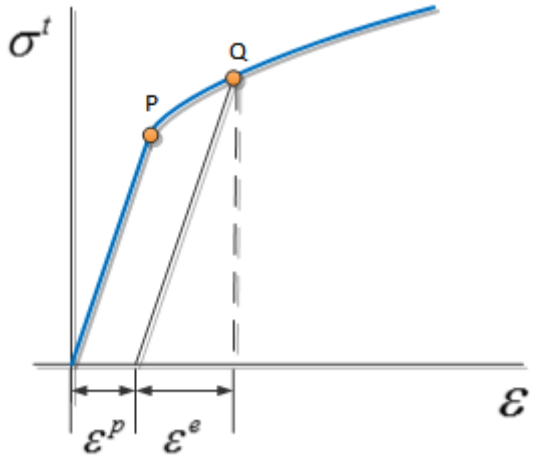

Fig. 2.3 Common true stress-true strain curve

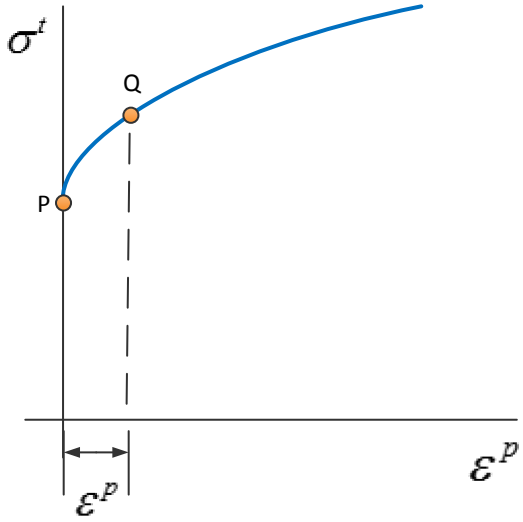

Fig. 2.4 Hardening curve obtained from true stress-true strain curve

Commonly non uniform hardening data after uniform deformation is extrapolated of hardening curve. There are several types of strain hardening functions such as Hollomon type, Ludwick type, Swift type, Voce type and Swift-Voce combined type.

$$\bar{\sigma} = K\bar{\varepsilon}^{n} \text{ : Hollomon type} \quad \textbf{(1.19)}$$

$$\bar{\sigma} = \bar{\sigma}_{y} + K\bar{\varepsilon}^{n} \text{ : Ludwick type} \quad \textbf{(1.20)}$$

$$\bar{\sigma} = K\left(\bar{\varepsilon} + \varepsilon_{0}\right)^{n} \text{ : Swift type} \quad \textbf{(1.21)}$$

$$\bar{\sigma} = A + B\left(1 - e^{-C\bar{\varepsilon}}\right) \text{ : Voce type} \quad \textbf{(1.22)}$$

$$\bar{\sigma} = K\left(\bar{\varepsilon} + \varepsilon_{0}\right)^{n} + C\left(1 - e^{-D\bar{\varepsilon}}\right) \text{ : Swift-Voce combined type} \quad \textbf{(1.23)}$$

Hollomon, Ludwick and Swift type can express monotone increasing behavior of stress. Voce type describes the convergent behavior upon some value. Swift-Voce combined type shows both features depending on its determined coefficients. However it can't present decreasing stress along the strain.

Chapter 3. Experiments

3.1 Test specimen

The clad material composed of stainless 316 affiliation (SUS316) and resistant corrosion metal was used in this studies. To prepare the specimen, wire-cut-E.D.M.(Electric Discharge Machining)method was carried out. Dimensions of the tensile specimen are shown in Fig. 3.1. The both sides of graspable portion by machine are 30mm and the radius of curvature is 8mm in between.

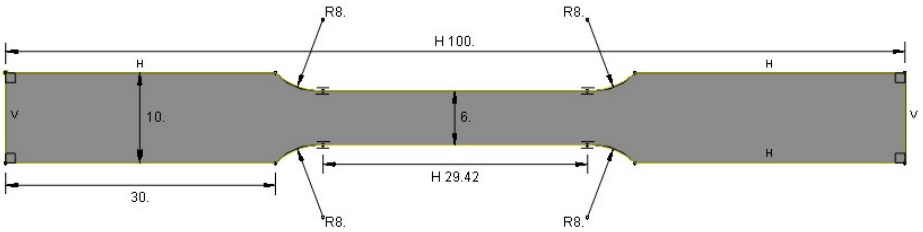

Fig. 3.1 Dimensions of the test specimen

After the specimen prepared, the sample was cut in the plane which is perpendicular to the welding direction to measure the material property of the clad through the thickness which is shown in Fig. 3.2. In the figure, the red colored parts are resistant corrosion metal and the others are SUS316. The coating near the surface is named as COAT-1 and near the interface with the base material is named as COAT-2. For the base material, totally four parts are obtained. Two are retained on the interface and another is retained on the

bottom of the clad and the other is located in the middle place. The Nearest base material on the interface is named SUS-3 and the next near base material on the interface SUS-4, the base located in the middle place SUS-5, the furthermost base from the interface SUS-6 respectively.

Each thickness of COAT and SUS are 1mm and 2mm respectively. Although the total thickness of the coating material is 3mm, the coating is obtained in 1mm thickness because material disappears during the wire-cut-E.D.M. method.

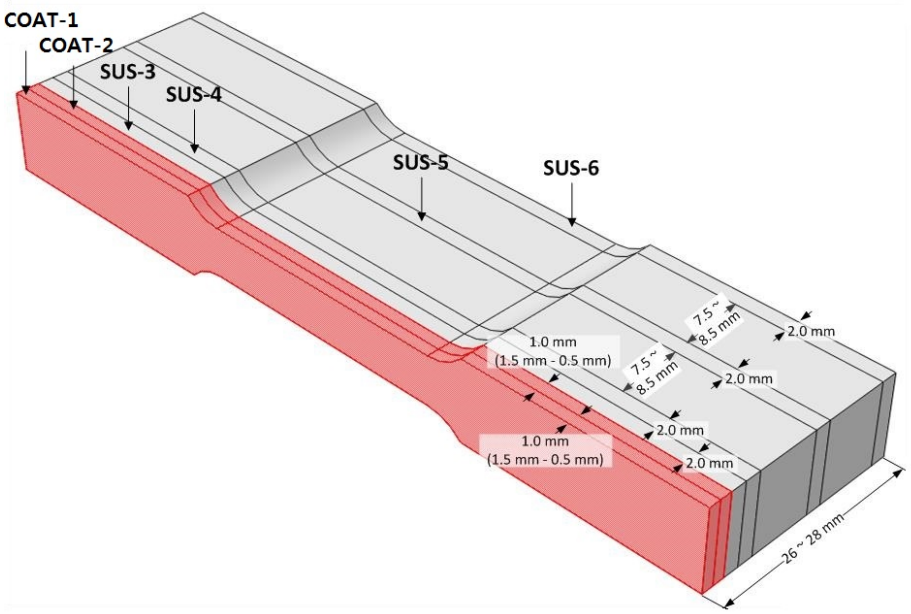

Fig. 3.2 Schematic positions of the each test specimens

3.2 Tester machine

To Analyze clad material section, uni-axial test was performed at room temperature and warm temperature which is 300℃. For the test, Instron 8801 universal testing machine was used that is shown in Fig. 3.3. The Load capacity is up to ±100kN. The crosshead speed ranges can be adjusted up to 1500mm/min. For the room temperature, the machine can be performed without any accessory.

Fig. 3.3 Instron 8801 universal testing machine set for room temperature experiment (the source of the Instron homepage: http://www.instron.co.kr)

When the test is conducted in warm temperature, the chamber which controls the temperature surrounding specimen is needed. As the test is performed in room temperature atmosphere, hydraulic grip was used without chamber. However when the test is performed in warm temperature, grip and specimen both were inside of chamber. The chamber can heats up temperature more than 300℃ blowing the warm air using the fan.

Fig. 3.4 Instron 8801 universal testing machine set for warm temperature experiment

3.3 Experiment method and conditions

Two isothermal conditions room temperature and 300℃ are concerned. Undergoing the experiments, thermometer was attached directly on the specimen to measure the exact temperature to avoid measuring surrounding temperature. When warm temperature 300℃ were targeted, the average temperature departure was retained ±3℃ compared to objective temperature.

The grip speed was determined on 0.032mm/sec to keep the engineering strain rate on approximate 0.001/sec. In order to take a strain measurement, extensometer and strain gauge were used. The maximum elongation of the extensometer is up to 50% and initial deformation was measured by strain gauge for accurate measurement.

Chapter 4. Results and Discussion

4.1 Simple tension results

Near the interface on which coating and stainless steel meet together, the extracted specimens are largely bent as one can see in the below Fig. 4.1. The interface is in between COAT-2 and SUS-3. All things taken together from this, residual stress have occurred during the explosive weld process. Therefore, the effect of residual stress on mechanical properties of clad material should be considered for deep investigation. However in this dissertation, the specimens are assumed as the virgin materials.

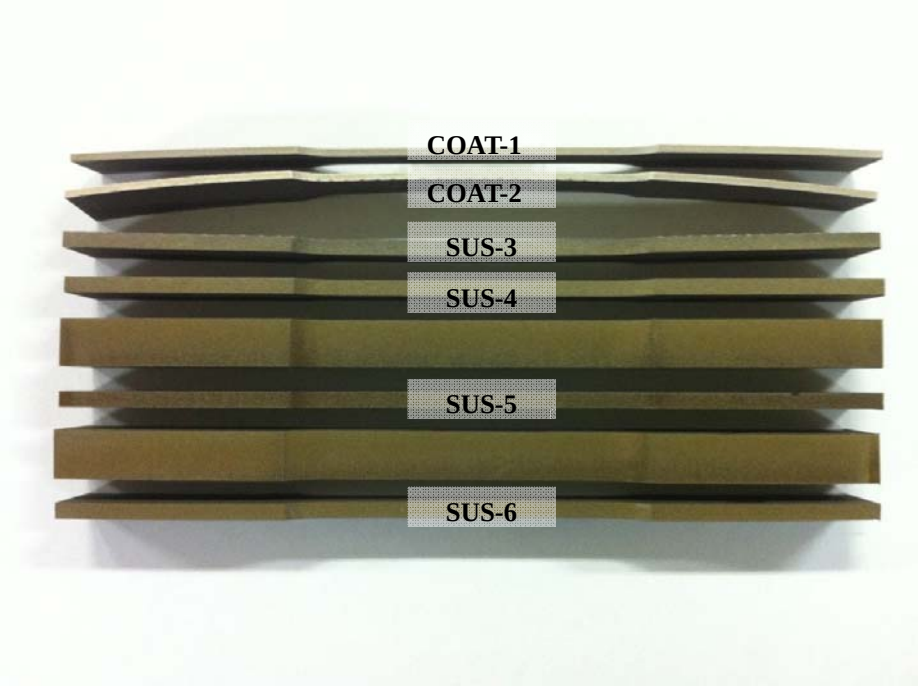

Fig. 4.1 Real positions of the each test specimens

4.2 Stress and Strain curve

Force and displacement of grip were directly obtained as a raw data at first time. However displacement is insufficient to express material behavior because the data obtained from the difference of grip holder contains non-uniform deformation region. To consider displacement only in the uniform deformation region, extensometer which has been already mentioned was used. Then, the engineering strain straightly comes out from extensometer. Engineering stress is calculated from the load cell force divided by initial area that was measured before the test.

The results of uni-axial test on the room temperature and 300℃ are shown in Fig. 4.2. The row-axis is engineering strain and the column-axis is engineering stress. To compare the extracted specimens through the thickness in same temperature, engineering stress-engineering strain curve is plotted for each temperature. For reference the nearest specimens to interface are COAT-2 and SUS-3. The nearer to the interface, the higher the strength of SUS. That is, the strength of SUS-3 is higher than that of SUS-4. At the same way, the strength of SUS-4 is higher than that of SUS-5 and that of SUS-5 is higher than that of SUS-6. However the more it is close to the interface, the more total elongation decreases close. This is the result of work hardening or strain hardening which comes from dislocation movement during explosive process. However there is no big difference for plot of COAT. Because the thickness of COAT is thinner than SUS specimen, COAT-1 and COAT-2 experience almost same level of work hardening.

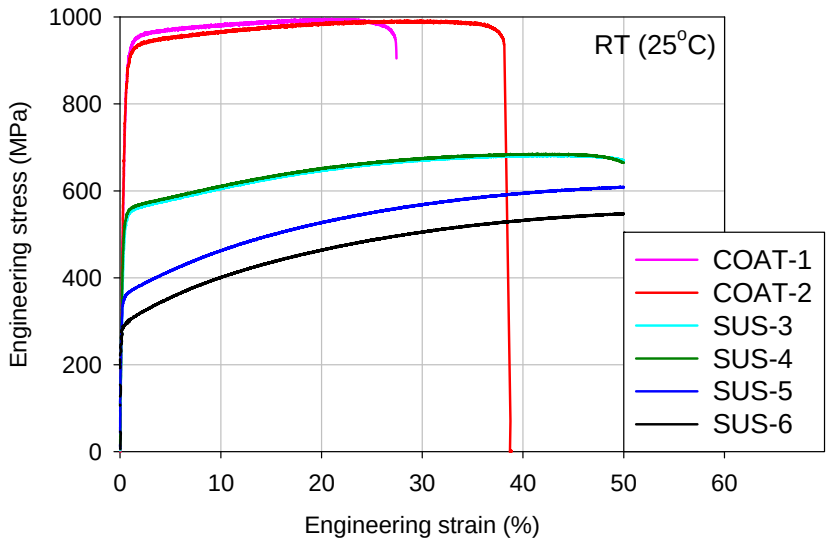

(a)

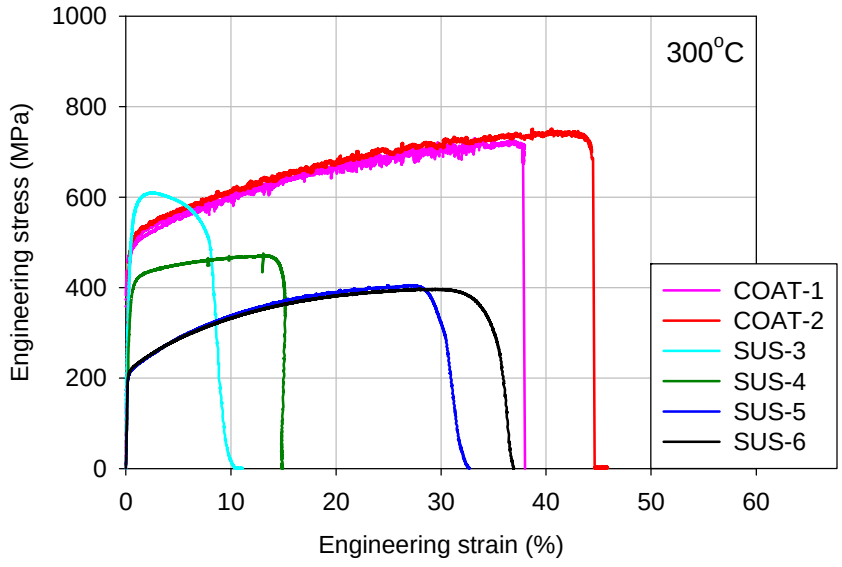

(b)

Fig. 4.2 Engineering stress-engineering strain curves for each temperature. (a) Room temperature, (b) 300℃

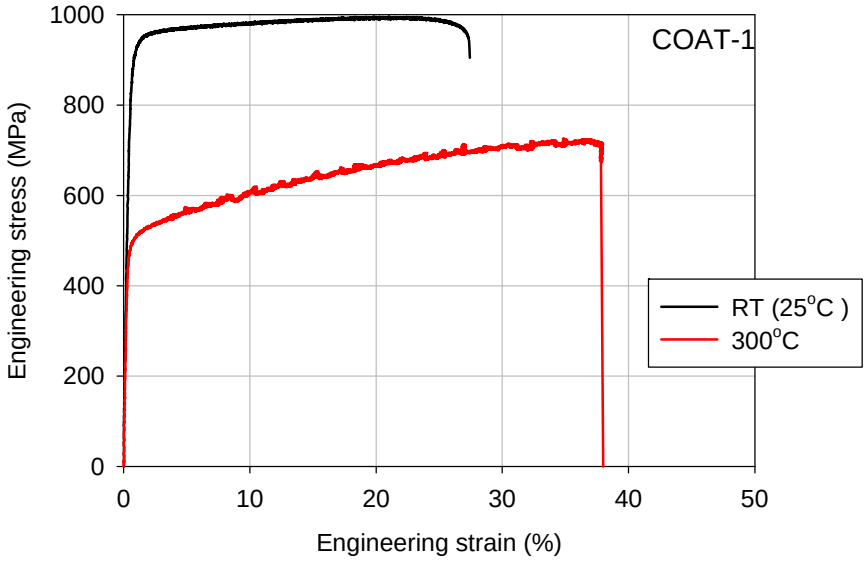
COAT-1
Engineering stress (MPa)
Engineering strain (%)
RT (25°C)
300°C
0
200
400
600
800
1000
0
10
20
30
40
50

(a)

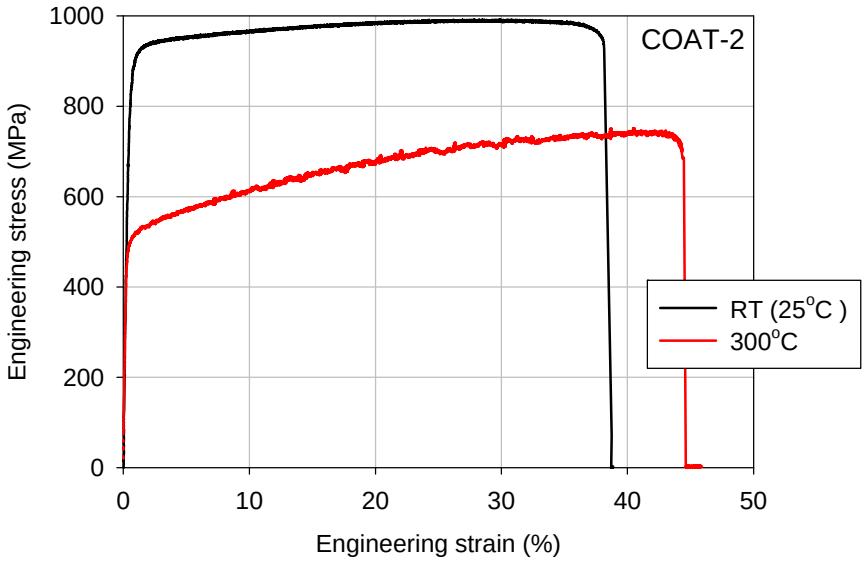
COAT-2
Engineering stress (MPa)
Engineering strain (%)
RT (25°C)
300°C
0
200
400
600
800
1000
0
10
20
30
40
50

(b)

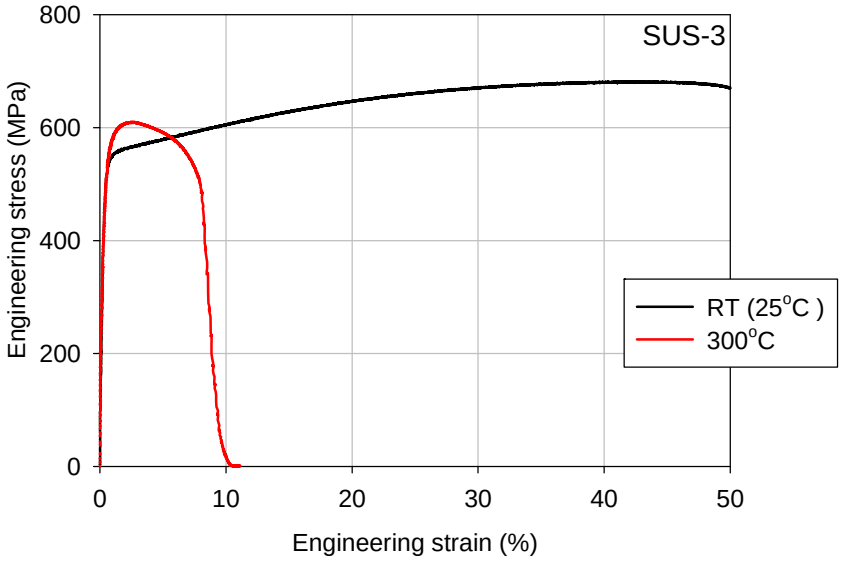
SUS-3
Engineering stress (MPa)
800
600
400
200
0
0
10
20
30
40
50
Engineering strain (%)
RT (25°C)
300°C

(c)

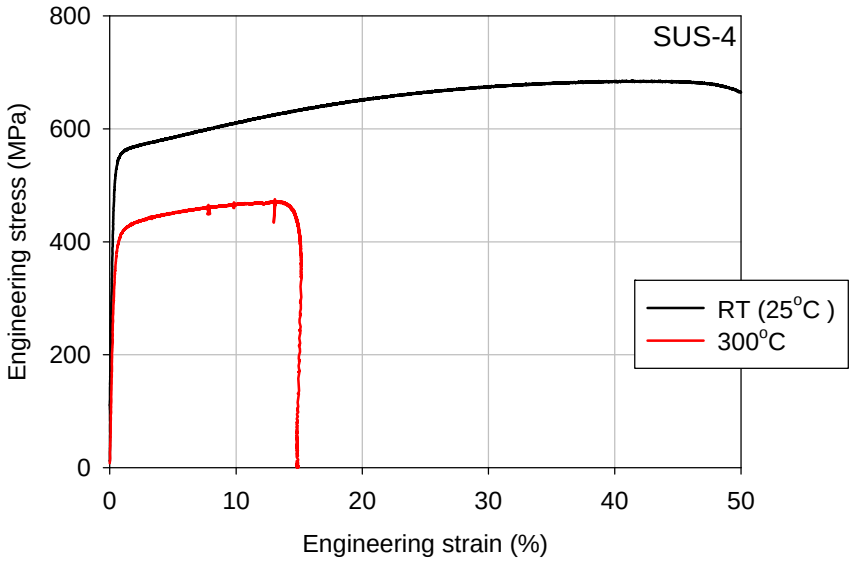
SUS-4
Engineering stress (MPa)
800
600
400
200
0
0
10
20
30
40
50
Engineering strain (%)
RT (25°C)
300°C

(d)

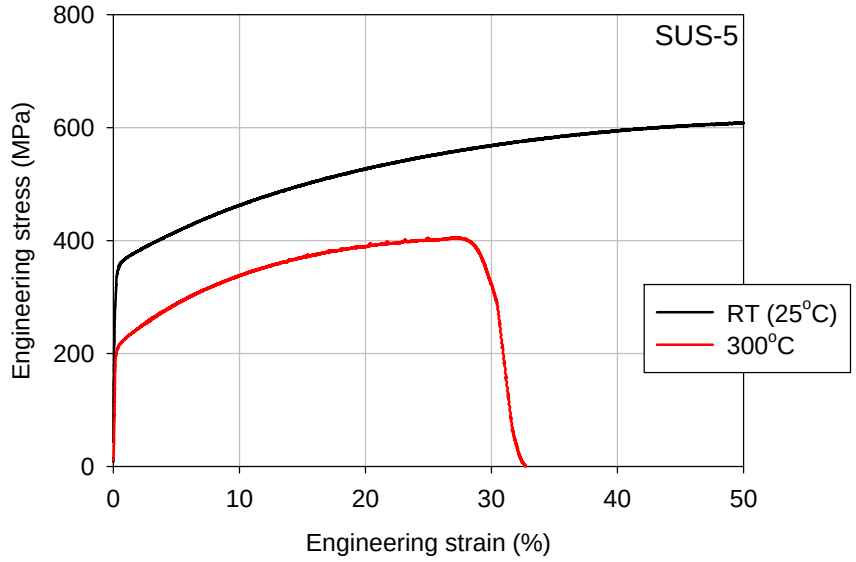

(e)

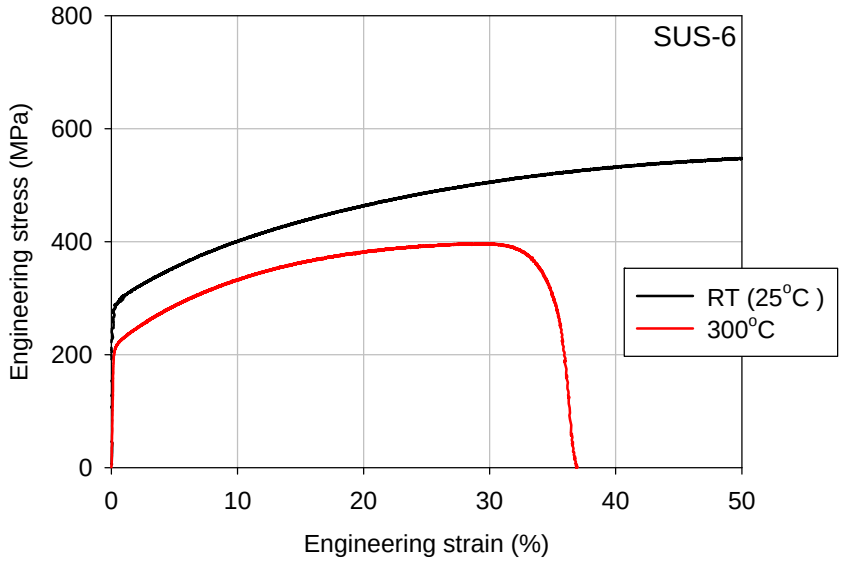

(f)

Fig. 4.3 Engineering stress-engineering strain curves for each location. (a) COAT-1, (b) COAT-2, (c) SUS-3, (d) SUS-4, (e) SUS-5, (f) SUS-6

4.3 Characteristics of the material

Elastic modulus was calculated from each stress-strain data. The elastic modulus are arranged in below Table 4.1. To measure yield stress and Young's modulus more accurately, strain gauges were employed. For each room temperature and 300℃, YFLA-2-1L, ZFLA6-11 models of strain gauge produced by Tokyo Sokki Kenkyujo company were used as simple tensile test was performed. YFLA-2-1L is used for room temperature and ZFLA6-11 is used for 300℃ respectively.

There is a tendency that elastic moduli decrease when the temperature goes higher. The Young's modulus of SUS-3 is lower than any other parts. This may be caused by the change of mechanical properties near the interface during the welding process.

	RT (25℃)	300℃
COAT-1	182.10	195.13
COAT-2	198.48	172.35
SUS-3	152.06	113.94
SUS-4	222.24	163.08
SUS-5	210*	179.82
SUS-6	210*	175.26

Table 4.1 Elastic modulus in engineering stress-engineering strain curve (unit: GPa)

** are referred from AISI stainless steel type316 properties* (the source of *http://www.efunda.com/glossary/materials/alloys/materials--alloys--steel--stainless_steel--aisi_type_316.cfm*)

After explosive process the clad welding conditions have big deviation from the extracted location. The bulk clad panel thickness has approximately ±1mm distance difference from location to location which is shown in the Fig. 4.4.

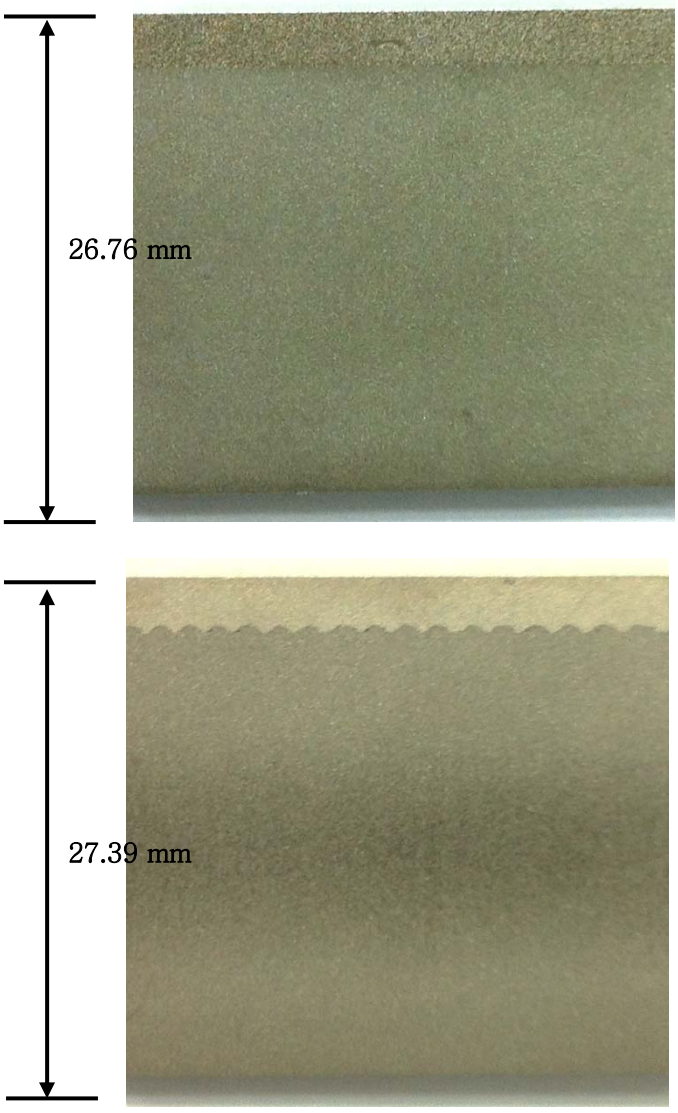

Fig. 4.4 Interface of the clad

The results of the uni-axial test at room temperature are arranged in Table 4.2 and Table 4.3. Those of test at 300℃ are arranged in Table 4.4 and Table 4.5. The thickness of specimen, the 0.2%-offset yield stress(YS), the ultimate tensile strength(UTS), the uniform elongation which is engineering strain when ultimate tensile strength occurs and the total elongation are retained from engineering stress-engineering strain curve arranged in Table 4.2 and Table 4.4. The 0.2%-offset yield stress(YS), the ultimate tensile strength(UTS), the uniform elongation which is true strain when ultimate tensile strength occurs are retained from true stress-true strain curve arranged in Table 4.3 and Table 4.5.

The strain was measured until 50% elongation because 50% elongation is the limit of extensometer's confident interval. The inequality expression '>' means that its value will be more than right hand side from the limitation of measurement cause.

Specimens	Thickness(mm)	*YS* (MPa)	*UTS* (MPa)	% Elongation	
				Uniform	Total
Room temperature (25℃)					
COAT-1	0.7597	875.40	992.81	20.75	27.43
COAT-2	0.8637	848.93	989.33	29.64	38.87
SUS-3	2.0273	522.04	680.80	42.78	>50
SUS-4	2.0300	531.82	684.13	41.51	>50
SUS-5	1.9017	346.61	> 608.36	>50	>50
SUS-6	1.9915	290.67	>548.06	>50	>50

Table 4.2 Plastic properties from engineering stress-engineering strain curve at room temperature

Specimens	*YS* (MPa)	*UTS* (MPa)	Uniform Elongation
Room temperature (25℃)			
COAT-1	882.17	1193.82	0.0187
COAT-2	855.01	1277.11	0.0260
SUS-3	525.46	967.38	0.0356
SUS-4	535.18	963.73	0.0347
SUS-5	347.98	>907.35	>0.050
SUS-6	292.93	>804.25	>0.050

Table 4.3 Plastic properties from true stress-true strain curve at room temperature

Specimens	Thickness(mm)	*YS* (MPa)	*UTS* (MPa)	% Elongation	
				Uniform	Total
Warm temperature (300℃)					
COAT-1	0.8570	489.54	768.11	43.46	45.89
COAT-2	0.8570	482.55	770.85	37.64	38.16
SUS-3	1.8997	545.93	609.37	2.56	11.01
SUS-4	2.0060	388.35	470.52	13.20	14.93
SUS-5	2.0048	209.10	404.68	27.06	32.63
SUS-6	2.0187	212.77	396.18	27.93	38.03

Table 4.4 Plastic properties from engineering stress-engineering strain curve at warm temperature (300℃)

Specimens	*YS* (MPa)	*UTS* (MPa)	Uniform Elongation
Warm temperature (300℃)			
COAT-1	491.81	1097.40	0.0361
COAT-2	485.27	1055.82	0.0320
SUS-3	550.66	622.53	0.0253
SUS-4	390.73	530.86	0.0124
SUS-5	209.89	512.28	0.0240
SUS-6	213.58	505.02	0.0246

Table 4.5 Plastic properties from true stress-true strain curve at warm temperature (300℃)

The Hardening curve can be obtained from the true stress-true strain curve. For room temperature, the hardening curves are fitted by Swift type. The coefficients of Swift hardening are shown in the Table 4.6. The curves are plotted in the Fig. 4.5.

RT	K (MPa)	ε_0	n
COAT-1	1714	0.2564	0.4348
COAT-2	1702	0.3875	0.6364
SUS-3	1354	0.1619	0.5060
SUS-4	1352	0.1602	0.4960
SUS-5	1261	0.0424	0.4362
SUS-6	1112	0.0269	0.4035

Table 4.6 Coefficients of the curves fitted by Swift type at room temperature

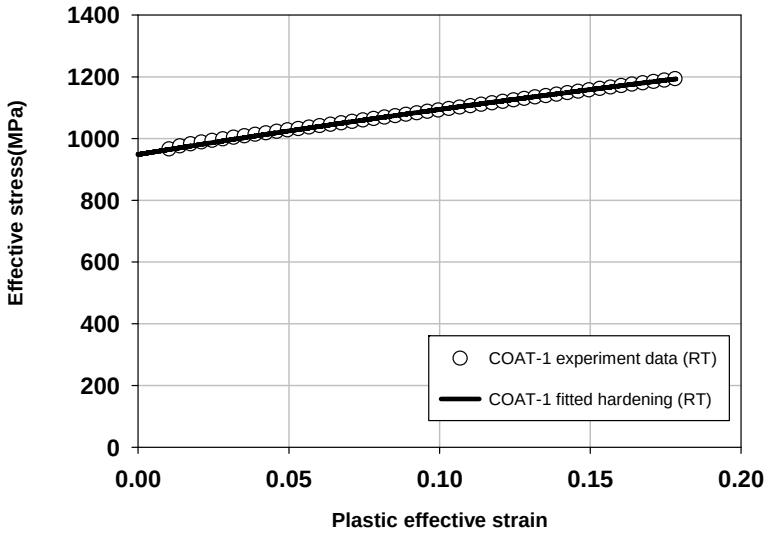
1400
1200
1000
800
600
400
200
0
Effective stress(MPa)
0.00
0.05
0.10
0.15
0.20
Plastic effective strain
COAT-1 experiment data (RT)
COAT-1 fitted hardening (RT)

(a)

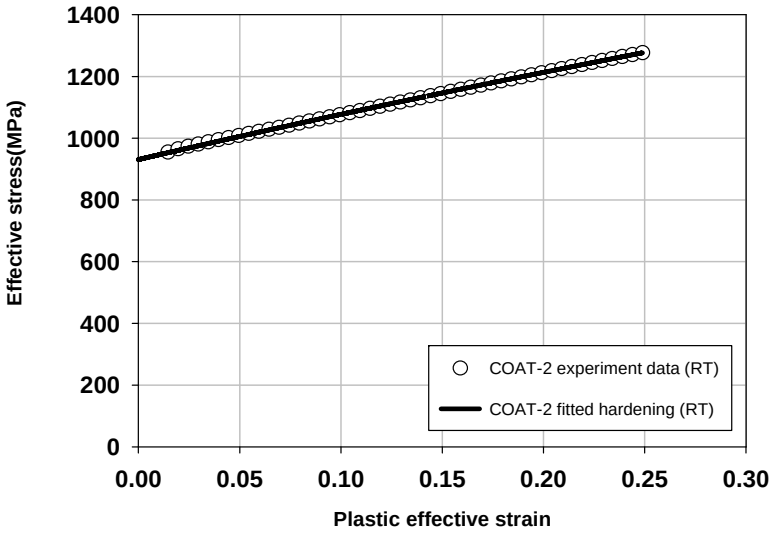
1400
1200
1000
800
600
400
200
0
Effective stress(MPa)
0.00
0.05
0.10
0.15
0.20
0.25
0.30
Plastic effective strain
COAT-2 experiment data (RT)
COAT-2 fitted hardening (RT)

(b)

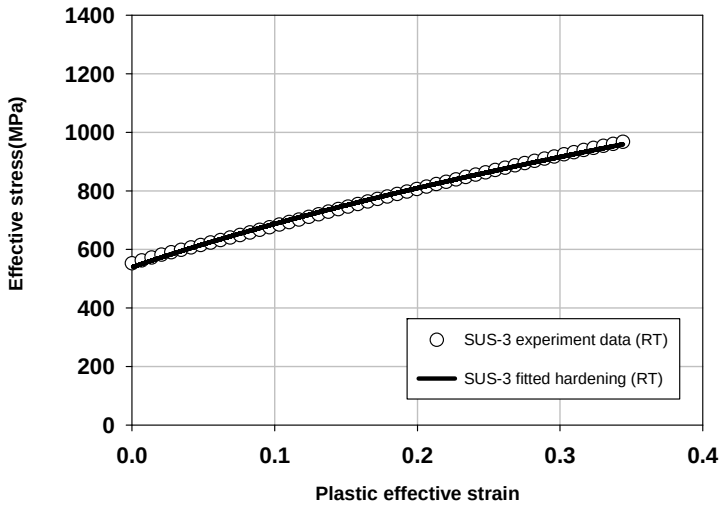
1400
1200
1000
800
600
400
200
0
Effective stress(MPa)
0.0
0.1
0.2
0.3
0.4
Plastic effective strain
SUS-3 experiment data (RT)
SUS-3 fitted hardening (RT)

(c)

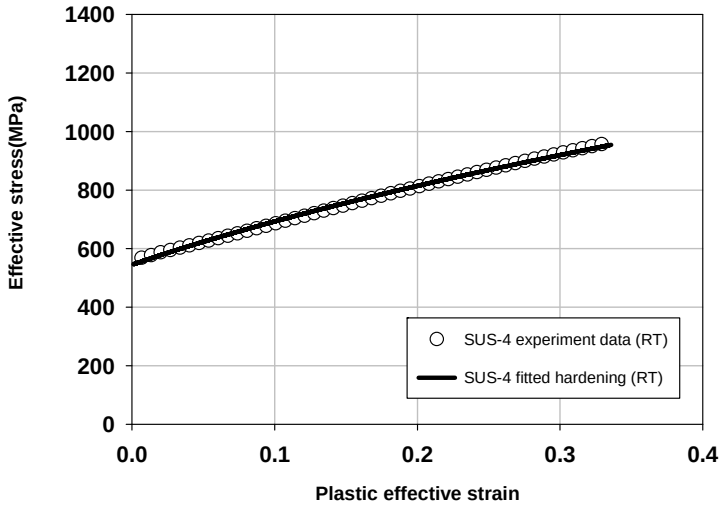
1400
1200
1000
800
600
400
200
0
Effective stress(MPa)
0.0
0.1
0.2
0.3
0.4
Plastic effective strain
SUS-4 experiment data (RT)
SUS-4 fitted hardening (RT)

(d)

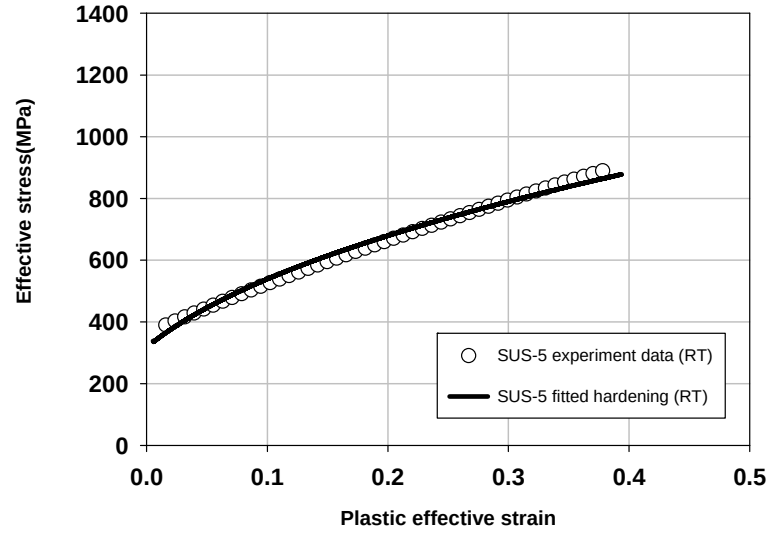

(e)

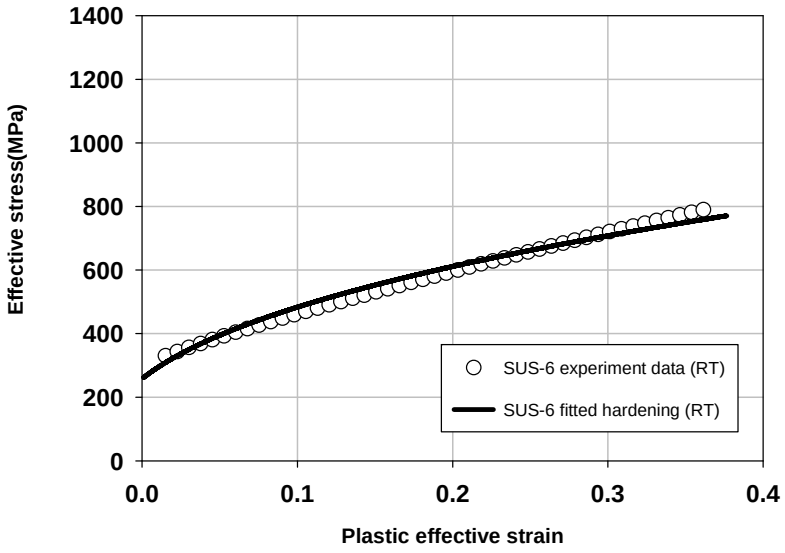

(f)

Fig. 4.5 Hardening curves fitted by Swift type at room temperature (a) COAT-1, (b) COAT-2, (c) SUS-3, (d) SUS-4, (e) SUS-5 (f) SUS-6

For 300℃, the hardening curves are also fitted by Swift type. The coefficients of Swift hardening are shown in the Table 4.7. The curves are plotted in the Fig. 4.6.

RT	K (MPa)	ε_0	n
COAT-1	1494	0.0680	0.4186
COAT-2	1383	0.0521	0.3594
SUS-3	659	0.0001	0.0156
SUS-4	694	0.0237	0.1394
SUS-5	679	0.0020	0.2322
SUS-6	676	0.0035	0.2409

Table 4.7 Coefficients of the curves fitted by Swift type at warm temperature (300℃)

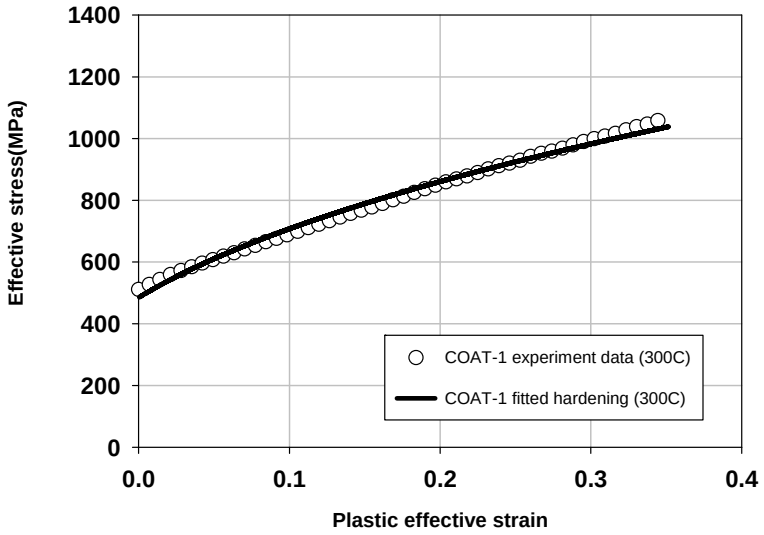
1400
1200
1000
800
600
400
200
0
Effective stress(MPa)
0.0
0.1
0.2
0.3
0.4
Plastic effective strain
COAT-1 experiment data (300C)
COAT-1 fitted hardening (300C)

(a)

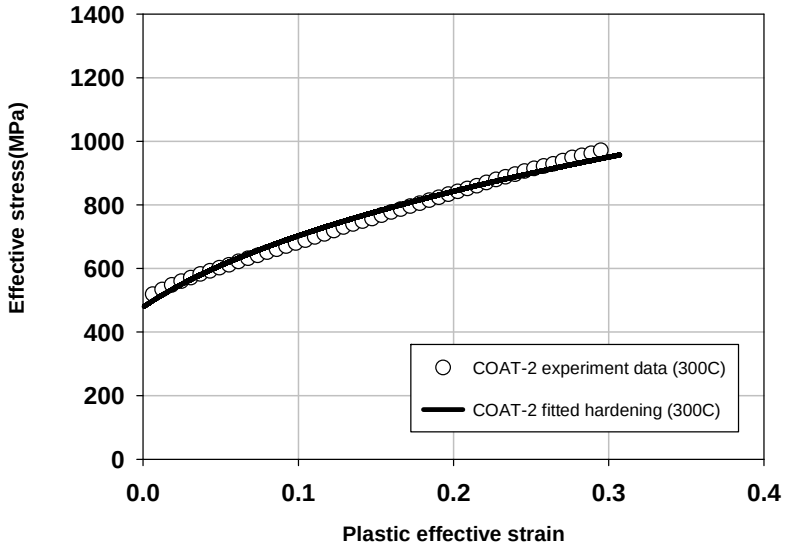
1400
1200
1000
800
600
400
200
0
Effective stress(MPa)
0.0
0.1
0.2
0.3
0.4
Plastic effective strain
COAT-2 experiment data (300C)
COAT-2 fitted hardening (300C)

(b)

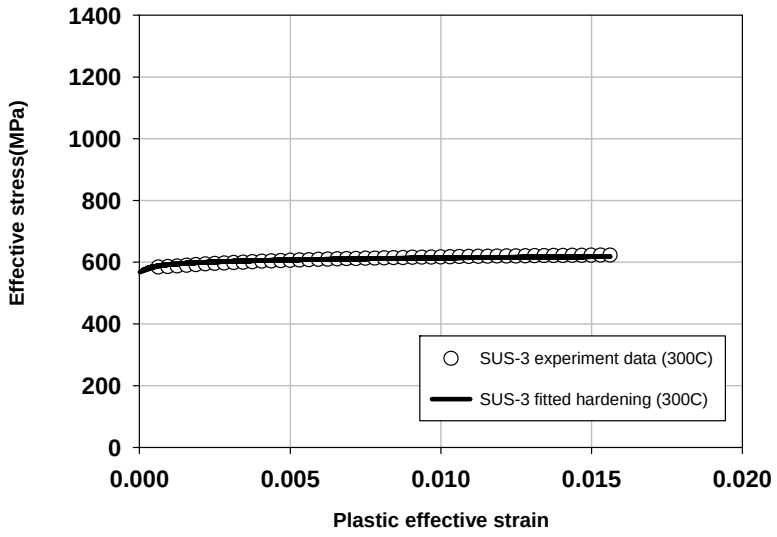
Effective stress(MPa)
1400
1200
1000
800
600
400
200
0
0.000
0.005
0.010
0.015
0.020
Plastic effective strain
SUS-3 experiment data (300C)
SUS-3 fitted hardening (300C)

(c)

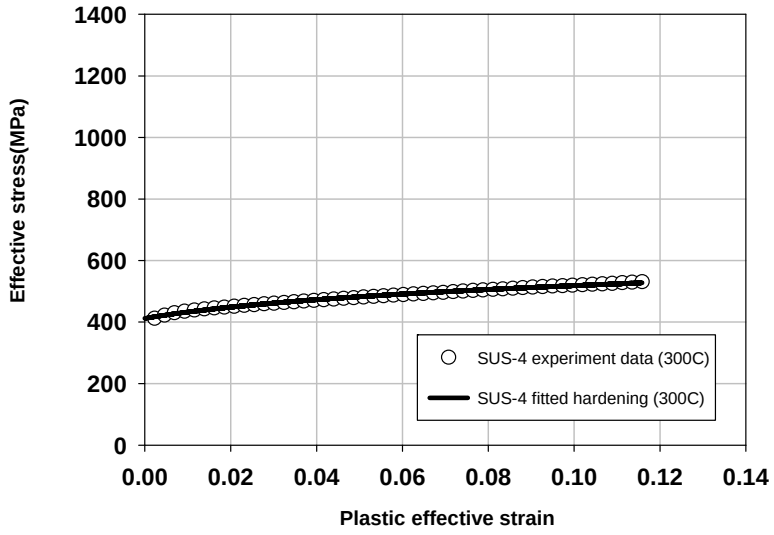
Effective stress(MPa)
1400
1200
1000
800
600
400
200
0
0.00
0.02
0.04
0.06
0.08
0.10
0.12
0.14
Plastic effective strain
SUS-4 experiment data (300C)
SUS-4 fitted hardening (300C)

(d)

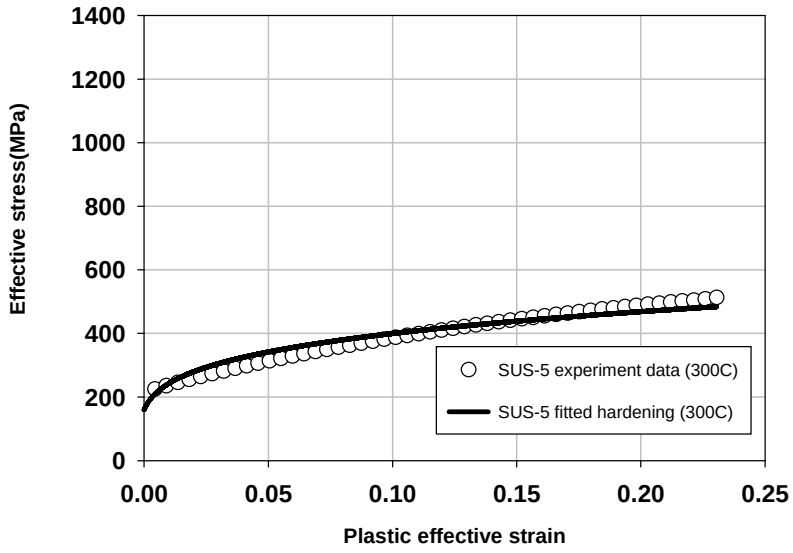

(e)

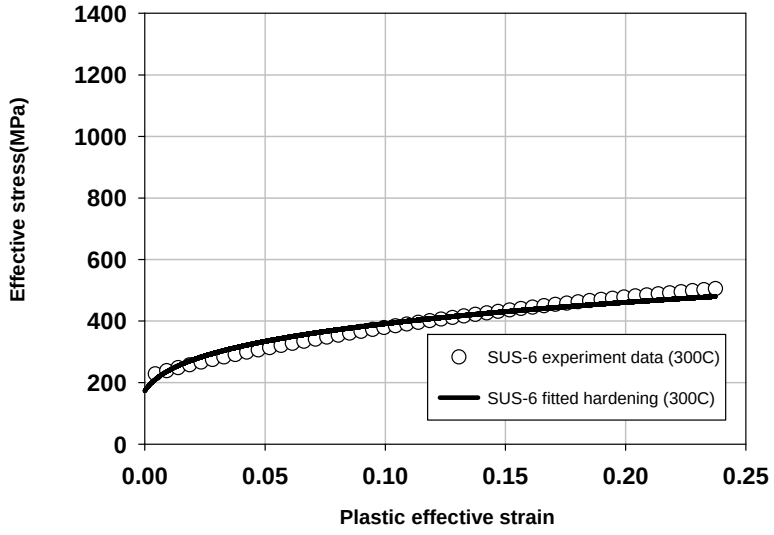

(f)

Fig. 4.6 Hardening curves fitted by Swift type at warm temperature (300℃) (a) COAT-1, (b) COAT-2, (c) SUS-3, (d) SUS-4, (e) SUS-5 (f) SUS-6

4.4 Verification

To perform the uni-axial test of the clad panel in whole thickness, unusual specimen design is devised for simple tensile test. The specimen design is illustrated in Fig. 4.7. The red colored part is coating and the other gray is stainless steel. In the middle the width is much longer than the grip width. However the thickness is reduced comparing to the other parts to concentrate the deformation on gauge length. The dimension of the specimen is shown in Fig. 4.8. Uni-axial tension were performed for this specimen at room temperature and 300℃.

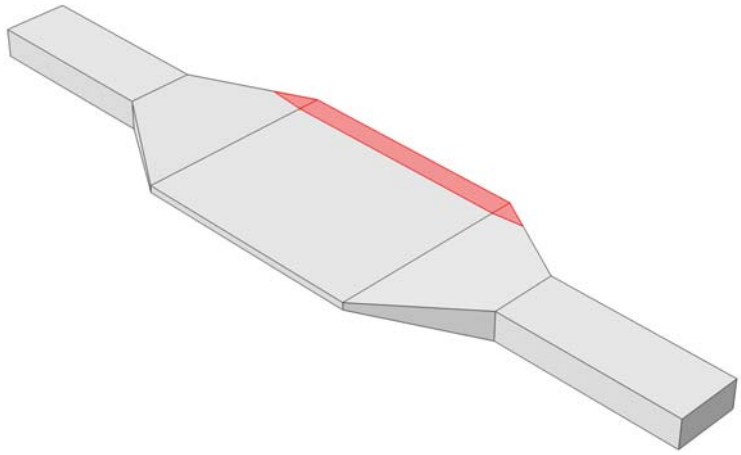

Fig. 4.7 Unusual specimen design for bulk clad material

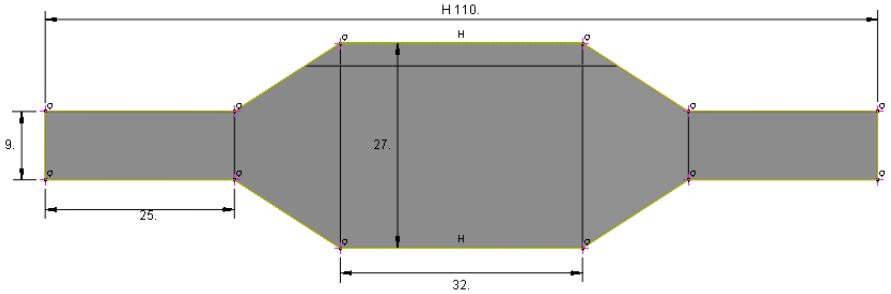

(a)

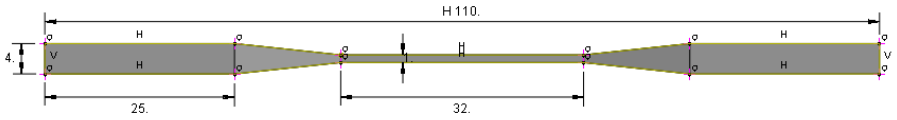

(b)

Fig. 4.8 The dimension of the unusual specimen (a) top view (b) side view

To predict the mechanical uni-axial behavior of the bulk clad material which were characterized before, the simulation program ABAQUS/Standard was used in this research. C3D8R which is an 8-node linear brick, reduced integration, hourglass control was used as the simulation element type. The Input density was 7.8 g / cm^3 , Poisson's ratio was 0.3 which is assumed value. The characterized materials were used in this simulation. The used Young's modulus are listed in Table 4.1. Isotropic hardening was used. The hardening stress of SUS-45 was an arithmetic mean of that of SUS-4 and SUS-5 and the hardening stress of SUS-56 was an average of SUS-5 and SUS-6.

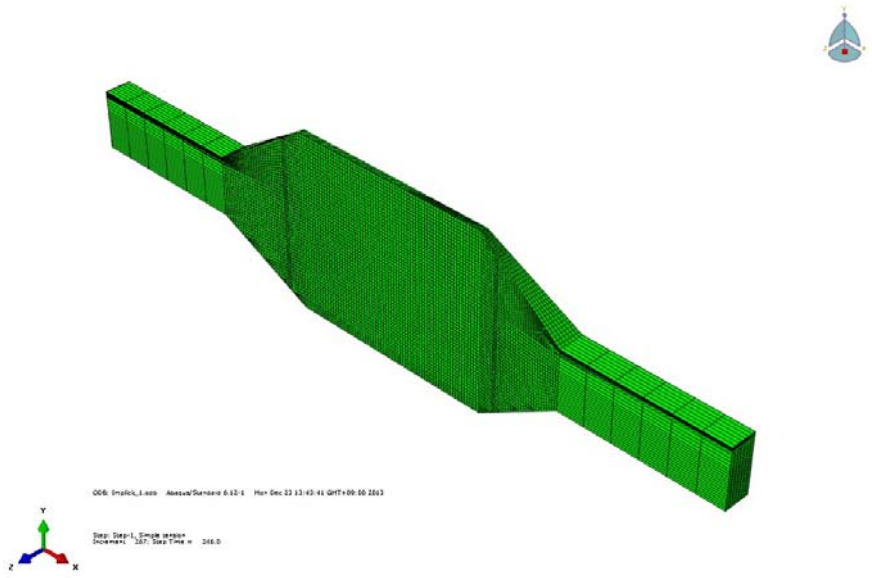

Fig. 4.9 Clad specimen in ABAQUS/Standard

The clad material is usually used as a structural material with experiencing warm temperature atmosphere. Only initial behaviors are interested for the structural metal. However to confirm the possibility to predict the plastic behavior of the bulk metal, the interested region is restricted up to 20% engineering strain elongation in both experiment and simulation. The uniform deformation limit of COAT-1 is the smallest comparing any other parts which is near 20% for room temperature roughly considered as instable behavior after it passes 20% elongation. On contrary SUS-3 in 300℃ has a very short uniform elongation limit only up to approximate 2%. However, without loss of generality, 20% was chosen for interested region at 300℃. And each results are shown in Fig. 4.10 and Fig. 4.11.

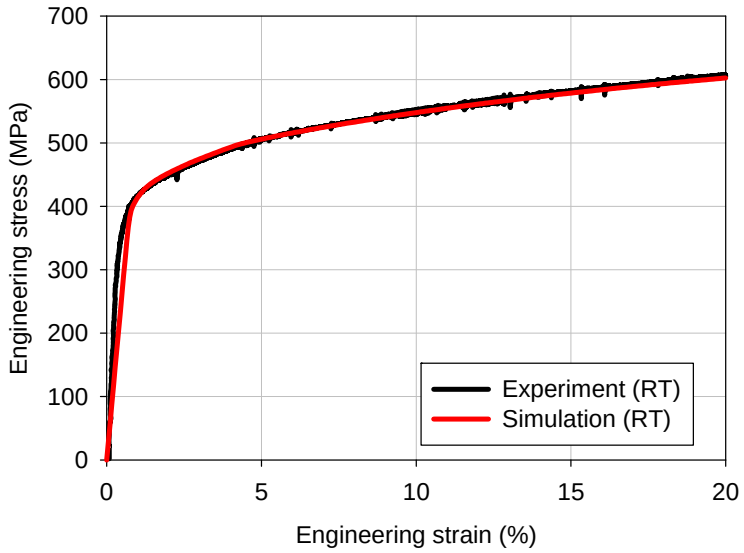

Fig. 4.10 Comparison simulation result with experiment at room temperature

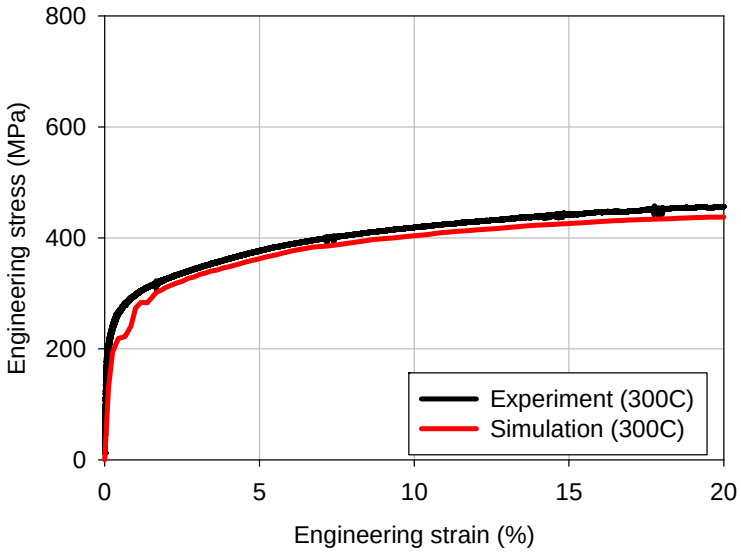

Fig. 4.11 Comparison simulation result with experiment at 300℃

Chapter 5. Conclusions

In this thesis, the uni-axial mechanical behavior of bulk clad material was compared with the simulation results predicting the whole behavior with using its partial properties.

Bulk clad is widely used as a structural material. So to predict its initial behavior and the magnitude of the yield point is important for its use. This is because only elastic ranges are usually researched as dealing with bulk clad material. However the further ranges are considered in this thesis. The plastic deformation until 20% elongation are predicted by locally partial material which is relatively easy to measure. As a results, partial properties of clad material well represent the whole mechanical behavior at both room temperature and warm temperature(300℃).

In this thesis, all partial materials are assumed as virgin materials which have never experienced any mechanical effect and there is no consideration of the interaction of unusual design specimen. For the sake of the more precise results, the interaction occurred by residual stress should be considered.

Bibliography

[1] R. Mendes, J. B. Ribeiro, and A. Loureiro, "Effect of explosive characteristics on the explosive welding of stainless steel to carbon steel in cylindrical configuration," *Materials & Design*, vol. 51, pp. 182-192, 10// 2013.

[2] C. Merriman, "The fundamentals of explosion welding," *Welding Journal (Miami, Fla)*, vol. 85, pp. 27-29, 2006.

[3] A. S. Khan and S. Huang, "Continuum theory of plasticity," pp. 4-7, 1995.

[4] R. Kacar and M. Acarer, "An investigation on the explosive cladding of 316L stainless steel-din-P355GH steel," Journal of Materials Processing Technology, vol. 152, pp. 91-96, 10/1/ 2004.

[5] R. Kaçar and M. Acarer, "Microstructure-property relationship in explosively welded duplex stainless steel-steel," Materials Science and Engineering A, vol. 363, pp. 290-296, // 2003.

[6] S. H. Choi, K. H. Kim, K. H. Oh, and D. N. Lee, "Tensile deformation behavior of stainless steel clad aluminum bilayer sheet," Materials Science and Engineering A, vol. 222, pp. 158-165, // 1997.

[7] B. K. Sarkar, M. K. Mukherjee, and A. Natarajan, "MODIFICATION OF THE RULE OF MIXTURE IN ESTIMATING STRENGTHSOF A COMPOSITE," Z WERKSTOFFTECH, vol. V 13, pp. 269-273, // 1982.

[8] S. L. Semiatin and H. R. Piehler, "Deformation of sandwich sheet materials in uniaxial tension," Metallurgical Transactions A, vol. 10, pp. 85-96, // 1979.

[9] R. V. Tamhankar and J. Ramesam, "Metallography of explosive welds," Materials Science and Engineering, vol. 13, pp. 245-254, 3// 1974.

[10] S. R. Reid, "A discussion of the mechanism of interface wave generation in explosive welding," International Journal of Mechanical Sciences, vol. 16, pp. 399-400, // 1974.

국문 초록

본 연구의 목적은 폭파용접으로 내부식성 코팅 재료와 스테인리스 스틸 모재료를 결합한 벌크 클래드 금속의 기계적 거동을 예측하는데 있다.

클래드 벌크의 기계적 인장 물성을 측정하기 위해 새로운 시편 디자인이 고안 되었다. 하지만 온간에서 견뎌야 하는 클래드 벌크 재료의 특성상 이 시편 디자인은 온도에 따라 변하는 재료의 물성을 제대로 표현할 수가 없다. 왜냐하면 폭파용접으로 인해 서로 다른 열 팽창계수를 갖는 재료가 용접 되어, 열해석시 발생하는 응력을 고려할 수 없기 때문이다. 이를 위해 재료를 두께별로 나누어 물성을 측정하였고, 이를 통해 클래드 전체의 역학적 거동을 예측해 보았다.

결과적으로 개별적 시편의 물성이 전체적인 역학적 거동을 짧은 변형 구간인 탄성영역뿐만 아니라 긴 변형 구간인 소성영역의 거동까지 상온과 온간에서 잘 예측함을 알 수 있다.

주요어: 폭파용접, 벌크, 클래드, 온간, 역학적 거동
학 번: 2012-20642